Approximate Two-Point Boundary Value Problem Solutions to Low Thrust Trajectory by Superposition

By Ming TONY Shing,[1)] Chit HONG Yam,[2)] and Albert WAI Kit Lau[1)]

[1)]*Department of Physics, Hong Kong University of Science and Technology, Hong Kong*
[2)]*ispace inc., Tokyo Japan*

(Received June 21st, 2017)

In the analysis on two-point boundary value problem of low thrust trajectories, solutions usually cannot be solved analytically. Rather the problem can only be analyzed through large amount of numerical optimization. We would like to seek for a shortcut to determine the solution of the trajectory under complex thrust profile. This report presents a new method to solve the 2D low thrust trajectories with multiple segments of thrust by combining solutions of single segment with constant thrust. This method has been applied to several test cases and the solutions are compared with raw data generated from grid search. The results have been found to be well matching with the raw data. This method may potentially be implement as standard method to include low-thrust trajectories in Lambert algorithm.

Key Words: low-thrust, Lambert problem, linearized method, superposition

Nomenclature

$\vec{r}$	:	Position vector
$\vec{v}$	:	Velocity vector
μ	:	Standard gravitational parameter = GM
$\mathcal{T}$	:	Time of flight
$\vec{u}_{[...]}(t)$	:	Thrust profile
n	:	Number of segment of thrust profile
U	:	Thrust magnitude
$\vec{u}_k$	:	Thrust vector during segment (t_{k-1}, t_k)
$\mathcal{U}$	:	Set of thrust vector
$\mathcal{V}$	:	Set of feasible velocity vector
$\vec{\delta}$	:	Position deviation from Lambert solution
$\vec{\delta v}$	:	Velocity deviation from Lambert solution
$\vec{\Delta}$	:	Error compared with grid search result
Subscripts		
i	:	Initial
f	:	Final
0	:	Lambert solution
x, y	:	Derivative in x, y direction
[...]	:	correspond to thrust profile [...]

1. Introduction

In celestial mechanics, the ballistic two-point boundary value problem, i.e. the Lambert Problem,[1)] can be solved analytically for a given transfer time, initial and final positions. The solutions to the Lambert problem are often expressed as the initial and final velocities. When generalizing the problem to low-thrust trajectories, one needs to search a range of feasible velocities of instead of discrete point solutions with computationally intensive approaches such as grid searches.[2)]

Previously a linearized method has been suggested to quickly compute the ranges of feasible velocities for low-thrust trajectories.[3)] However such method fails in long duration orbits. In this paper, we have developed a new method to approximate the feasible velocity ranges of a low-thrust trajectory with complex thrust profile using solutions of trajectories with simple thrust profile. Firstly the problem is formulated as follow: (1) The thrust profile $\vec{u}(t)$ is parametrized to a sum of constant pulse function, indicating the thrust direction on each segment of the trajectory. (2) The pulse on each segment can be turn on or off. Then the feasible velocity ranges can be spanned via grid search of all combination of thrust direction and magnitude.

However such method is very time consuming. To reduce the number of computations, we explore patterns in the solutions generated from grid search - the feasible range of trajectories with multiple thrust-ed segments can be approximated by sum of the feasible ranges of trajectories with single thrust-ed segment, i.e. a superposition of solutions to simpler thrust profile yields the solution of more complex thrust profile. This approximation scheme has been applied to several test cases and successfully reproduces the feasible range in long orbit predicted by grid search. The analytical basis of this method will also be discussed briefly.

Solving the two-point boundary value problem of low-thrust trajectories efficiently can be very useful for the design of future low-thrust missions. Mapping the final velocity range of the current orbit with initial velocity range of the next orbit allows faster and more accurate prediction during a large scale tree search of multi-leg trajectories and can result in better solutions consuming less propellant. With the succeed of this approximation method, we can improve the efficiency of low-thrust trajectory design by reducing number of computation from order $O(N^k)$ to $O(kN)$. It also allows extension to the standard ballistic Lambert algorithm to include low thrust trajectories.

2. Problem Statement

2.1. Lambert Problem

In orbital mechanics, the ballistic two-point boundary value problem is often referred as the Lambert Problem. The problem requires one to find the specific trajectory $\vec{r}(t)$ from the given initial position $\vec{r}_i$, final position $\vec{r}_f$ and transfer time $\mathcal{T}$. For sim-

plicity, we only consider the trajectories in 2D which surround a central body at $(0,0)$ with standard gravitational parameter μ. The equation of motion of such trajectory can be solved from the equation of motion under Newtonian gravitation

$$\frac{d^2}{dt^2}\vec{r}(t) = -\frac{\mu}{\left\|\vec{r}(t)\right\|^3}\vec{r}(t) \tag{1}$$

together with a given boundary conditions

$$\begin{cases}\vec{r}(0) = \vec{r}_i \\ \vec{r}(\mathcal{T}) = \vec{r}_f\end{cases} \tag{2}$$

The solution to the Lambert problem is often expressed in the form of the pair of initial velocity $\vec{v}(0) = \vec{v}_{0i}$ and final velocity $\vec{v}(\mathcal{T}) = \vec{v}_{0f}$. The analytical method to the solution can be found in many textbook on trajectories design.

2.2. Low Thrust Trajectories

In low thrust trajectory, Eq.(1) is modified by adding the thrust profile $\vec{u}(t)$ to give Eq.(3).

$$\frac{d^2}{dt^2}\vec{r}(t) = -\frac{\mu}{\left\|\vec{r}(t)\right\|^3}\vec{r}(t) + \vec{u}(t) \tag{3}$$

The thrust profile at different time interval are usually chosen to be different function. Denoting the thrust function in time interval (t_{k-1}, t_k) to be $\vec{u}_k(t)$, so that the indexing of a specific thrust profile on the whole trajectory can be displayed as $[\vec{u}_1(t), \vec{u}_2(t), ...\vec{u}_n(t)]$. By these notations, the complete thrust profile as a function of time can be expressed as

$$\vec{u}(t) = \vec{u}_{[12...n]}(t) = \sum_{k=1}^{n} \vec{u}_k(t)\left(H((t-t_{k-1}) - H(t-t_k)\right) \tag{4}$$

where $H(t)$ is the Heaviside function,[4] defined by

$$H(t) = \begin{cases}0 & \text{if } t \le 0 \\ 1 & \text{if } t > 0\end{cases} \tag{5}$$

Similar to ballistic Lambert problem, the solution is also commonly expressed in the form of initial and final solution. Suppose we choose each $\vec{u}_k(t)$ from a finite set of function $\mathcal{U}$ (e.g. the set of all thrust function with a particular constant magnitude U) to form all combination of thrust profile. The solutions to the low thrust trajectory of all these possible thrust profiles are expected to form the sets of feasible velocities $(\mathcal{V}_i, \mathcal{V}_f)$, denoting initial and final velocity sets respectively.[5] These sets of feasible velocities are expected to map out a range around the solution to the Lambert problem, as shown in Fig.1.

Solving Eq.(3) will give us the wanted low thrust trajectory and hence the initial and final velocity. However in most of the cases, there are no analytical solution and numerical methods are required. Therefore mapping out the complete, accurate sets of feasible velocity requires grid search on all combination of thrust profiles and is rather inefficient.

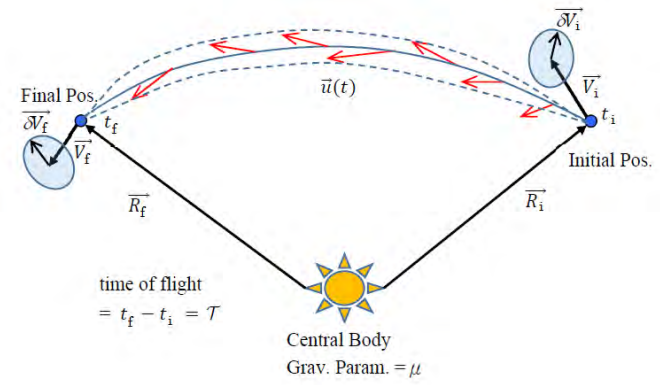

Fig. 1.: Schmetic to low thrust boundary value problem in trajectory design. The two light blue regions represent the set of feasible initial and final velocity respectively.

2.3. Method of Superposition

2.3.1. Idea

In our analysis, we would like to suggest a new method to approximate the solution to low thrust trajectories with complex thrust profile by combining those with simple thrust profile. To demonstrate, we work on two dimensional trajectories with magnitude of the thrust profile $\left\|\vec{u}(t)\right\|$ = constant. This is because the effectiveness of the approximation highly depends on the magnitude of the control.

The method of superposition makes use of the property of the Heaviside function and approximates the solution based on the Lambert solution. First, rewrite Eq.(3) in terms of x-y coordinate to give

$$\begin{cases}\dfrac{d^2}{dt^2}x(t) = u_x - \dfrac{x(t)}{\left(x(t)^2 + y(t)^2\right)^{3/2}} \\ \dfrac{d^2}{dt^2}y(t) = u_y - \dfrac{y(t)}{\left(x(t)^2 + y(t)^2\right)^{3/2}}\end{cases} \tag{6}$$

where $\vec{r}(t) = (x(t), y(t))$ is the coordinate of the low thrust trajectory. As we can see from Fig.1, under small thrust, the low thrust trajectory (dotted blue lines) can be approximated from the Lambert trajectory (solid blue line) by adding a small deviation. Therefore we may write $\vec{r}(t) = \vec{r}_0(t) + \vec{\delta}(t) = (x_0(t) + \delta x(t), y_0(t) + \delta y(t))$, where $(x_0(t), y_0(t))$ is the coordinate of the Lambert trajectory. Then expand Eq.(6) upon $(x_0(t), y_0(t))$ to give

$$\begin{cases}\dfrac{d^2}{dt^2}\delta x &= u_x + \left(F_x\delta x + F_y\delta y\right) \\ &\quad + \dfrac{1}{2}\left(F_{xx}(\delta x)^2 + 2F_{xy}(\delta x)(\delta y) + F_{yy}(\delta y)^2\right) \\ &\quad + \{\text{higher order terms}\} \\ \dfrac{d^2}{dt^2}\delta y &= u_y + \left(G_x\delta x + G_y\delta y\right) \\ &\quad + \dfrac{1}{2}\left(G_{xx}(\delta x)^2 + 2G_{xy}(\delta x)(\delta y) + G_{yy}(\delta y)^2\right) \\ &\quad + \{\text{higher order terms}\}\end{cases} \tag{7}$$

where

$$F = -\frac{x_0}{(x_0^2+y_0^2)^{3/2}}, \quad G = -\frac{y_0}{(x_0^2+y_0^2)^{3/2}} \tag{8}$$

are time-dependent function solely depend on the Lambert trajectory.

Suppose we bisect the trajectory by transfer time, so that the thrust profile contains only two components $[\vec{u}_1, \vec{u}_2]$. Notice that from the defined control function from Eq.(4), the control function $\vec{u}_{[12]}$ to the thrust profile $[\vec{u}_1, \vec{u}_2]$ can be written as the sum of the control function $\vec{u}_{[1]}$ from profile $[\vec{u}_1, 0]$ and control function $\vec{u}_{[2]}$ from profile $[0, \vec{u}_2]$ due to the property of the Heavisde function, as shown in Fig.(2).

We denote the trajectory deviation under thrust profile $\vec{u}_{[1]}$ as $(\delta x_{[1]}, \delta y_{[1]})$, $\vec{u}_{[2]}$ as $(\delta x_{[2]}, \delta y_{[2]})$ and $\vec{u}_{[12]}c$ as $(\delta x_{[12]}, \delta y_{[12]})$. Substituting to the x-equation in Eq.(7) yields

$$\begin{cases} \frac{d^2}{dt^2}\delta x_{[1]} &= u_{x,[1]} + \left(F_x \delta x_{[1]} + F_y \delta y_{[1]}\right) \\ &\quad + \frac{1}{2}\left(F_{xx}(\delta x_{[1]})^2 + 2F_{xy}(\delta x_{[1]}\delta_{[1]} + F_{yy}(\delta y_{[1]})^2\right) \\ &\quad + \{\text{higher order terms}\} \\ \frac{d^2}{dt^2}\delta x_{[2]} &= u_{x,[2]} + \left(F_x \delta x_{[2]} + F_y \delta y_{[2]}\right) \\ &\quad + \frac{1}{2}\left(F_{xx}(\delta x_{[2]})^2 + 2F_{xy}(\delta x_{[2]}\delta y_{[2]}) + F_{yy}(\delta y_{[2]})^2\right) \\ &\quad + \{\text{higher order terms}\} \\ \frac{d^2}{dt^2}\delta x_{[12]} &= u_{x,[12]} + \left(F_x \delta x_{[12]} + F_y \delta y_{[12]}\right) \\ &\quad + \frac{1}{2}\left(F_{xx}(\delta x_{[12]})^2 + 2F_{xy}(\delta x_{[12]}\delta y_{[12]}) + F_{yy}(\delta y_{[12]})^2\right) \\ &\quad + \{\text{higher order terms}\} \end{cases} \tag{9}$$

From the definition of thrust profile in Eq.(4), $u_{x,[12]} = u_{x,[1]} + u_{x,[2]}$ by the property of step function. This hints that we may add the first two differential equations in Eq.(9) to construct a similar differential equation to the third one. Therefore it is possible that we may take $\delta x_{[12]} \approx \delta x_{[1]} + \delta y_{[2]}$, and similar in y direction. Such approximation is expected to work well if quadratic and higher order terms of the differential equations can be neglected.

Differentiating $\vec{\delta}_{[12]} \approx \vec{\delta}_{[1]} + \vec{\delta}_{[2]}$, we can then deduce that the deviation of the feasible initial and final velocities from the Lambert solution would also be similar: by obtaining the solution $\delta\vec{v}_{[1]}$ and $\delta\vec{v}_{[2]}$ corresponding to the thrust profile $[\vec{u}_1, 0]$ and $[0, \vec{u}_2]$, we can quickly approximate the solution $\delta\vec{v}_{[12]}$ corresponding to the thrust profile $[\vec{u}_1, \vec{u}_2]$ by $\vec{\delta v}_{[12]} \approx \vec{\delta v}_{[1]} + \vec{\delta v}_{[2]}$.

In general, such approximation can be extend to n segment cases. i.e. for the solution δ from the thrust profile $[\vec{u}_1, \vec{u}_2, ...\vec{u}_n]$ can be approximated by $\vec{\delta v}_{[12...n]} \approx \vec{\delta v}_{[1]} + \vec{\delta v}_{[2]} + ... + \vec{\delta v}_{[n]}$. This approximation scheme is thus called the method of superposition.

2.3.2. Criterion

The criterion that we may linearize the differential equation is that (2nd order terms) $\ll$ (1st order terms). Calculating all the 1st and 2nd order terms from Eq.(8):

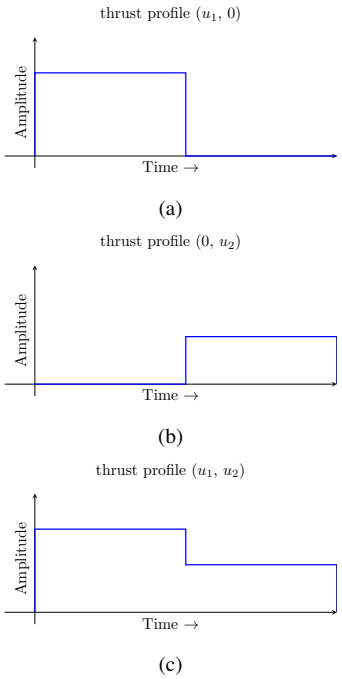

Fig. 2.: Plot of control functions against time for thrust profiles: (a):$(u_1, 0)$, (b):$(0, u_2)$ and (c):(u_1, u_2). Notice the control function from (u_1, u_2) be written as the sum of that of $(u_1, 0)$ and $(0, u_2)$.

$$\begin{cases} F_x \delta x = \dfrac{2x_0^2 - y_0^2}{\|r\|^4}\left(\dfrac{\delta x}{\|r\|}\right) \\ F_y \delta y = \dfrac{3x_0 y_0}{\|r\|^4}\left(\dfrac{\delta y}{\|r\|}\right) \end{cases} \tag{10}$$

$$\begin{cases} F_{xx}(\delta_x)^2 = \dfrac{9x_0y_0^2 - 6x_0^3}{\|r\|^5}\left(\dfrac{\delta x}{\|r\|}\right)^2 \\ F_{yy}(\delta_y)^2 = \dfrac{3x_0(x_0^2 - 4y_0^2)}{\|r\|^5}\left(\dfrac{\delta y}{\|r\|}\right)^2 \\ F_{xy}\delta x\delta y = \dfrac{3y_0(y_0^2 - 4x_0^2)}{\|r\|^5}\left(\dfrac{\sqrt{\delta x \delta y}}{\|r\|}\right)^2 \end{cases} \tag{11}$$

where$\|r\| = \sqrt{x_0^2 + y_0^2}$. We can show that the higher order terms form a series of $\left(\frac{\delta}{\|r\|}\right)$. Therefore the criterion for the approximation is $O\left(\frac{\delta}{\|r\|}\right) \ll 1$

We may then constrain the size of δ from the differential equation. As $\delta \ll \|r\|$ is likely valid only if the control function acts as a "perturbation force" to the gravitational force (see Eq.(1)), i.e. $\left\|\vec{u}\right\| \ll \frac{\mu}{\|\vec{r}\|^2}$. It suggests that the approximation for a control function with constant magnitude is better when the orbit is closer to the central body.

3. Numerical Examples

To demonstrate the effectiveness of the method of superposition, we have run many test cases using superposition and compared the mapped feasible velocity range to the results from grid search, and only some of them are shown here as examples.

We have chosen *bvp4c* from Matlab to approximate each solution of the two-pint boundary value problem. We only compare the results to trajectories divided up to 3 segments, and only demonstrate examples of two dimensional problems since this approximation scheme can be easily extended to more-segment cases and three dimensional problems.

For the grid search, we exhaust all the combination of thrust profile $[\vec{u}_1, \vec{u}_2, ...\vec{u}_n]$. Each $\vec{u}_k = (u_{k,x}, u_{k,y})$ are chosen to be $(0, 0)$ or $(U\cos(\frac{2\pi}{20}i), U\sin(\frac{2\pi}{20}i))$ with $i = 1, 2, ...20$, i.e. for each segment, there is either zero thrust or a constant thrust with magnitude U and angle $\frac{2\pi}{20}i$, total 21 possibilities. Then for a trajectory divided into n segments, the number of total possible combination of thrust profile would be 21^n. The plot of the results from grid search for all of these thrust profile are expected able to trace out the shape of the feasible velocities ranges.

In all of the trials, we have taken $\mu = 1$, $\vec{v}_i = (10, 0)$, $U = 10^{-4} \ll \frac{\mu}{\|\vec{r}\|} \approx 10^{-2}$. Transfer time is expressed in unit of $T = 2\pi\sqrt{\frac{10^3}{\mu}} \approx 198.69$ which is the time for traveling one complete circle of radius 10. Such transfer time is chosen so that the trajectories have low eccentricity and thus the method of superposition is always valid. On each plot of the feasible ranges, each feasible solution from one of the combination of thrust profile is displayed as one data point. The Lambert solution is displayed as a black cross, so each $(\delta\vec{v}_x, \delta\vec{v}_y)$ is visible as the distance between each data point and the black cross.

In the following sections, we demonstrate two cases: (i) $\vec{v}_f = (-2, 8)$, $\mathcal{T} = \frac{1}{3}T$; (ii) $\vec{v}_f = (-1, -9)$, $\mathcal{T} = \frac{2}{3}T$.

3.1. n = 2

The feasible velocity ranges plot for both cases (i) and (ii) are shown in Fig.3 and Fig.4 respectively.

Observe that for case (i), the solutions to the profile type $[\vec{u}_1, 0]$ (i.e. $\delta\vec{v}_{[1]}$)are distributed as a blue ellipse, while solutions to the profile type $[0, \vec{u}_2]$ (i.e. $\delta\vec{v}_{[2]}$) are distributed as a red ellipse around the Lambert solution. Solutions to the profile type $[\vec{u}_1, \vec{u}_2]$ (i.e. $\delta\vec{v}_{[12]}$) are shown as the green data points, which form a lot of small ellipse surrounding the Lambert solution. The pattern is less obvious for case (ii), although outlining all the small green ellipses is possible.

By further checking, in the plot of feasible initial velocity range, we can observe that the dimensions of the green ellipses are approximately equal to the red ellipse, and its center is approximately lying at one of the blue dot. Therefore we may trace out the outline of the feasible velocity ranges by: 1. Use the dimension of blue ellipse to trace out the locations of the center of green ellipses; 2. "Superposition" the center of red ellipses on the edge of the blue ellipse; 3. Translate the red ellipse around the blue ellipse to get the outline of the range. For the plot of feasible final velocity range, the procedure is similar except we superposition the blue ellipse onto the red ellipse instead.

This is in fact the results from the method of superposition: Dimensions of the blue ellipse are from the set of $\delta\vec{v}_{[1]}$, while those of the red ellipse are from the set of $\delta\vec{v}_{[2]}$. Therefore all of their combination give the approximation to the the location of all green dots $\delta\vec{v}_{[12]}$, i.e. $\delta\vec{v}_{[12]} \approx \delta\vec{v}_{[1]} + \delta\vec{v}_{[2]}$.

We can verify the effectiveness of the method of superposition by calculating the error $\vec{\Delta} = \delta\vec{v}_{[12]} - (\delta\vec{v}_{[1]} + \delta\vec{v}_{[2]})$. The results are plotted in Fig.5 and Fig.6. The errors for the two cases are found to be $\left\|\vec{\Delta}\right\| < 5 \cdot 10^{-5}$ and $\left\|\vec{\Delta}\right\| < 5 \cdot 10^{-4}$ respectively.

3.2. n = 3

The feasible velocity ranges for $n = 3$ to the two cases are plotted in Fig.7 and Fig.8. The situation is similar to $n = 2$ except that there are three layers of ellipses instead of two: Solutions to the profile type $[\vec{u}_1, 0, 0]$ (i.e. $\delta\vec{v}_{[1]}$)are distributed as a blue ellipse; Solutions to the profile type $[0, \vec{u}_2, 0]$ (i.e. $\delta\vec{v}_{[2]}$) are distributed as a red ellipse; Solutions to the profile type $[0, 0, \vec{u}_3]$ (i.e. $\delta\vec{v}_{[3]}$) are distributed as a green ellipse; Solutions to the profile type $[\vec{u}_1, \vec{u}_2, \vec{u}_3]$ (i.e. $\delta\vec{v}_{[123]}$) are shown as the yellow data points.

The coverage of the yellow area by smaller ellipses is not obvious due to too many data points. Yet the superposition $\delta\vec{v}_{[123]} \approx \delta\vec{v}_{[1]} + \delta\vec{v}_{[2]} + \delta\vec{v}_{[3]}$ is still applicable. The error $\vec{\Delta} = \delta\vec{v}_{[12]} - (\delta\vec{v}_{[1]} + \delta\vec{v}_{[2]} + \delta\vec{v}_{[3]})$ are also plotted in Fig.9 and Fig.10 for the two cases respectively. The magnitude of the error is found to be $\left\|\vec{\Delta}\right\| < 5 \cdot 10^{-6}$ and $\left\|\vec{\Delta}\right\| < 5 \cdot 10^{-4}$ respectively.

3.3. n > 3 and Extension of usage

Although we cannot work out the the solution for all combination for case $n > 3$ due to limitation of computational power, we can predict results of grid search for $n > 3$ by observing the behavior of $n = 1$ to 3.

From Fig.11 and Fig.12, we can see that the outline of the feasible velocity ranges can be roughly approximate by the results using n = 1. For larger n, there are extra solution lying at the peak of the elongated shape of the range, but the increment tends to converge. We expect that superposition for cases of larger n can still over the increment as it works in the cases $n = 1$, $n = 2$, and $n = 3$.

As the number of segment increases, we can use the control function $\vec{u}_{[12...n]}$ to approximate continuous functions. It means that for any given control function (not necessary written in the form of Eq.(4)), we can first approximate it into a summation of Heaviside functions and use method of superposition to find its corresponding initial and final velocity. This suggests that we can have a larger freedom of choice of control functions in trajectory design.

4. Conclusion

In this paper, we have introduced the approximation scheme "method of superposition". This method allows us to reduce amount of computation greatly to map out the feasible velocities set for the two-point boundary value problem of low thrust trajectory: Instead of applying grid search to all combination of thrust profile in the form of $[\vec{u}_1, \vec{u}_2, ..., \vec{u}_k]$, we can span the complete feasible velocity ranges by approximation using solutions to profiles $[0, ...0, \vec{u}_i, 0, ...0]$. For pratical usage, we usually set the number of choice of thrust angle to $20 \sim 30$, while number of segment as ~ 10. Thus The implement of the method of superposition could reduce the number of computation from $\sim 10^{14}$ to ~ 300, which is highly efficient. However the calculation also showed that this approximation is expected working particular well only when $\left\|\vec{u}_k\right\| \ll -\frac{\mu}{\|\vec{r}\|}$, i.e. when the trajectory is close to the central body.

The inclusion of this approximation scheme into the standard

ballistic Lambert algorithm can accelerate the search of multi-leg trajectories in low thrust mission design: feasible velocity ranges of legs can be computed more efficiently and used to determine smoothness at transfer between legs. Future work may focus on improving the approximation scheme so that it works for mission involving far orbits.

References

1) Bate, R. R., Muller, D. D. and White, J. E.,: *An Introduction to Astrodynamics*, Dover Publication, New York, 1971, Chapter 5.
2) Yam, C. H., Campagnola, S., Kawakatsu, Y. and Shing, M. T.,: *Feasibility Regions of Boundary Value Problems of Low-Thrust Trajectories*, 26th AAS/AIAA Space Flight Mechanics Meeting, Napa, CA, U.S.A., Feb, 2016, AAS paper 16-519.
3) Campagnola, S., Ozaki, N., Funase, R., Nakasuka, S., Sugimoto, Y., Yam, C.H., Kawakatsu, Y., Chen, H., Kawabata, Y., Ogura, S., and Sarli, B.,: *Low-thrust trajectory design and operations of PROCYON, the first deep-space micro-spacecraft*, 66th International Astronautical Congress (IAC2015), IAC-15-C1.1.8, Jerusalem, Israel, 2015.
4) Ernst, J. B.,: *Heaviside's Operational Calculus, as applied to Engineering and Physics*, McGraw-Hill Education, New York, 1936, pp5.
5) Heimonen, H. and Yam, C. H.,: *Analysis on the Solutions of Boundary Value Problems in Low-Thrust Trajectories*, 30th International Symposium on Space Technology and Science, June 2013.

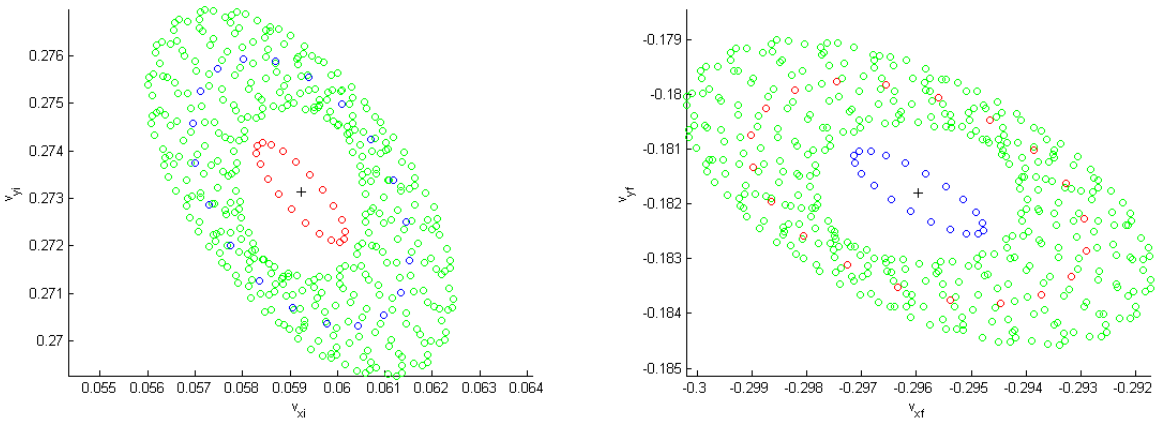

(a) (b)

Fig. 3.: Feasible initial (left) and final (right) velocity ranges for case (i): $\vec{v}_f = (-2, 8)$, $\mathcal{T} = \frac{1}{3}T$ with $n = 2$.

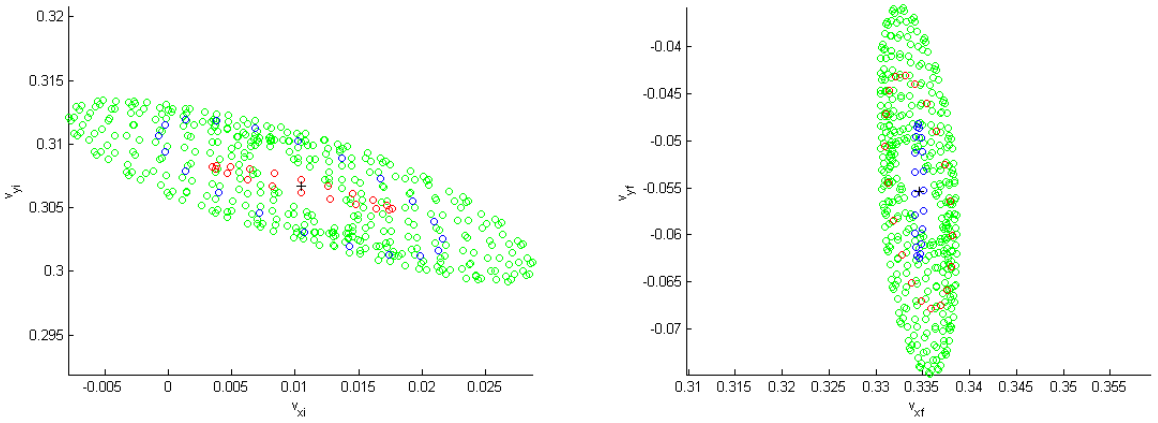

(a) (b)

Fig. 4.: Feasible initial (left) and final (right) velocity ranges for case (ii): $\vec{v}_f = (-1, -9)$, $\mathcal{T} = \frac{2}{3}T$ with $n = 2$.

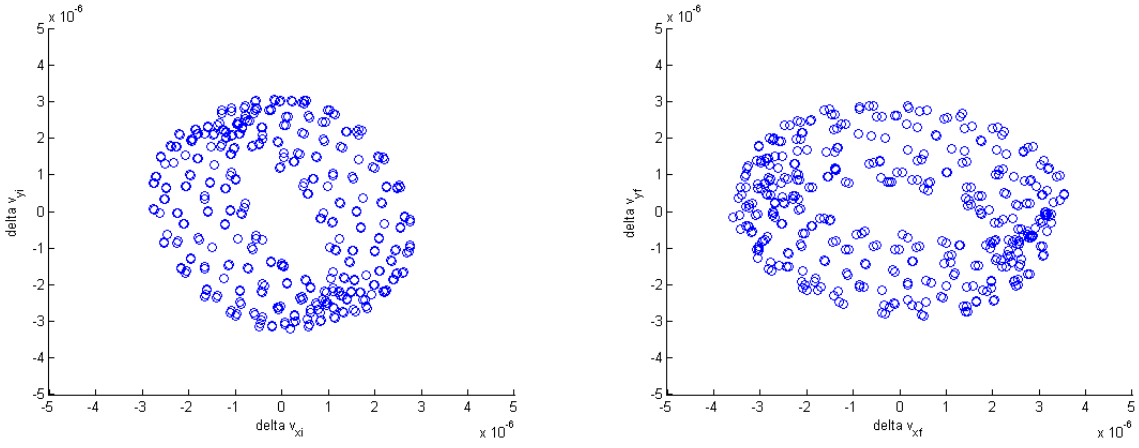

(a) (b)

Fig. 5.: Error between $\vec{\delta v}_{[12]}$ and $\vec{\delta v}_{[1]} + \vec{\delta v}_{[2]}$ for Case (i) at $n = 2$. Left: Initial velocity range; Right: Final velocity range.

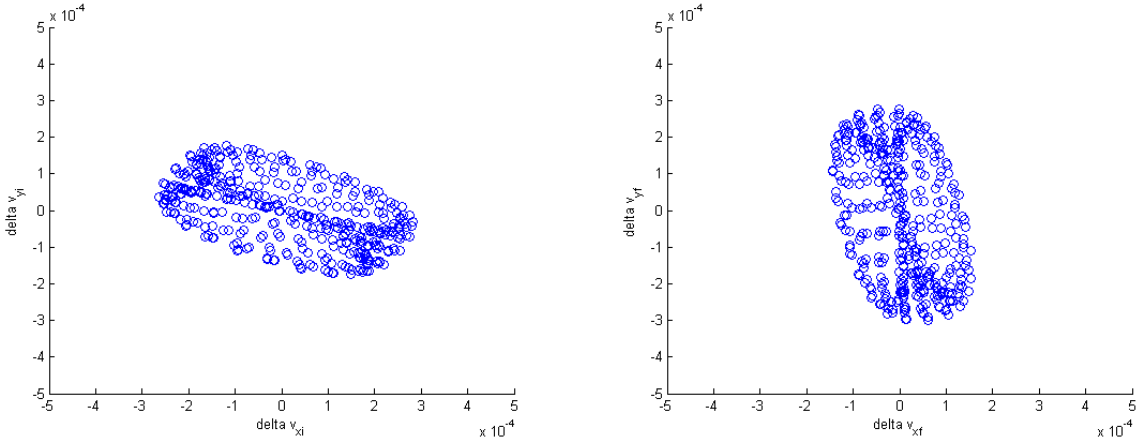

(a) (b)

Fig. 6.: Error between $\vec{\delta v}_{[12]}$ and $\vec{\delta v}_{[1]} + \vec{\delta v}_{[2]}$ for Case (ii) at $n = 2$. Left: Initial velocity range; Right: Final velocity range.

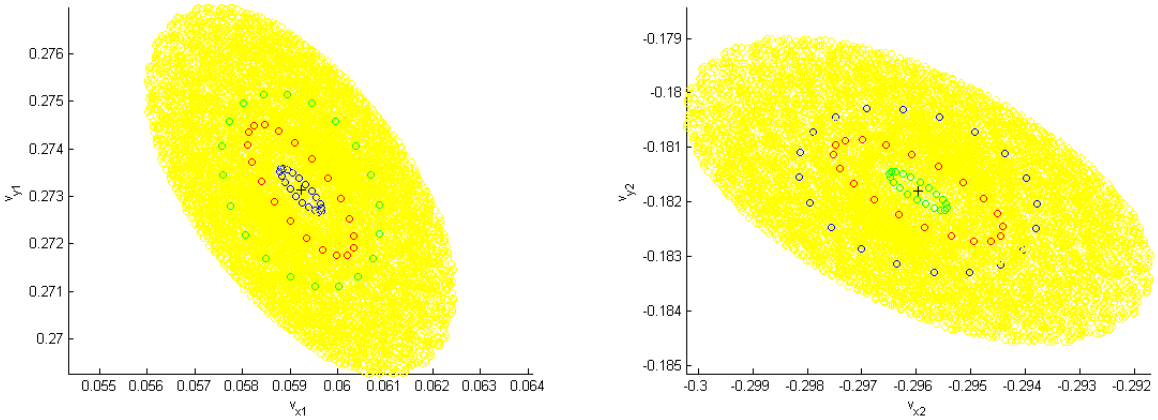

(a) (b)

Fig. 7.: Feasible initial (left) and final (right) velocity ranges for case (i): $\vec{v}_f = (-2, 8)$, $\mathcal{T} = \frac{1}{3}T$ with $n = 3$.

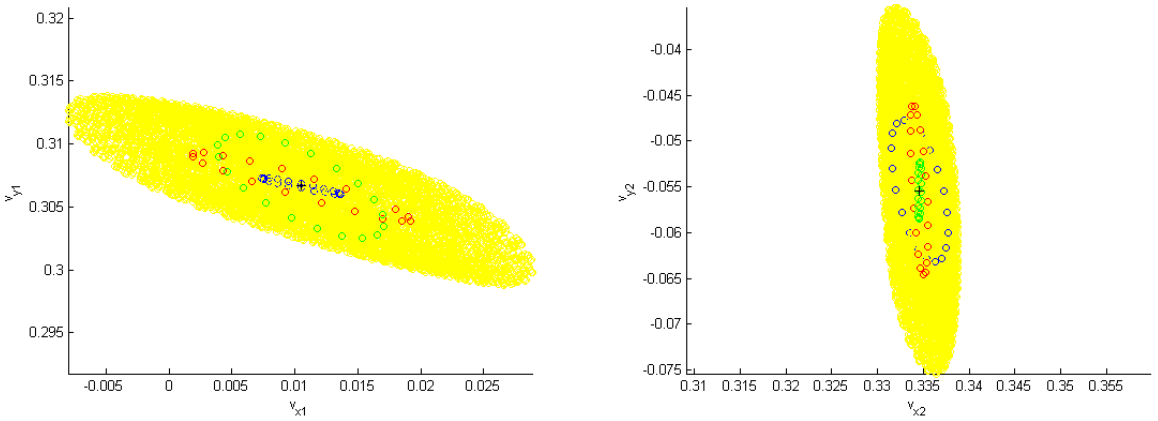

(a) (b)

Fig. 8.: Feasible initial (left) and final (right) velocity ranges for case (ii): $\vec{v}_f = (-1, -9)$, $\mathcal{T} = \frac{2}{3}T$ with $n = 3$.

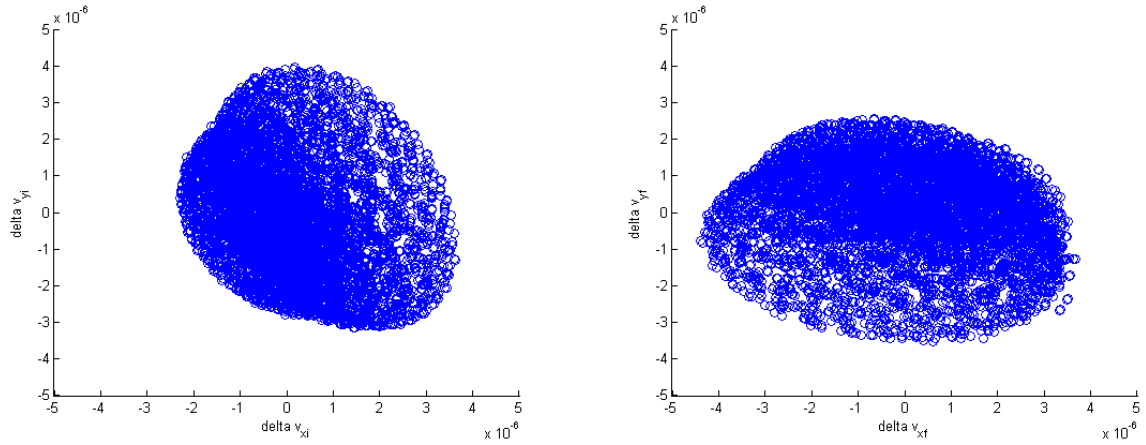

(a) (b)

Fig. 9.: Error between $\vec{\delta v}_{[123]}$ and $\vec{\delta v}_{[1]} + \vec{\delta v}_{[2]} + \vec{\delta v}_{[3]}$ for Case (i) at $n = 3$. Left: Initial velocity range; Right: Final velocity range.

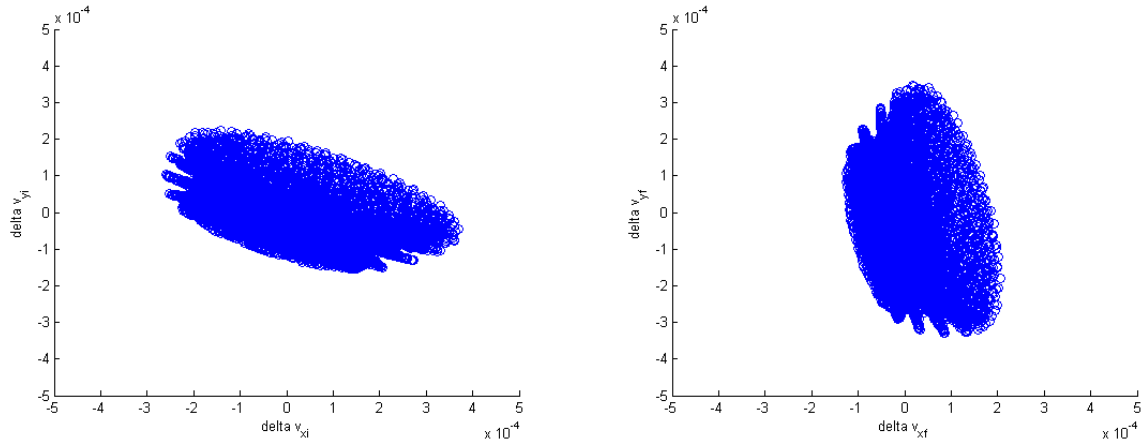

(a) (b)

Fig. 10.: Error between $\vec{\delta v}_{[123]}$ and $\vec{\delta v}_{[1]} + \vec{\delta v}_{[2]} + \vec{\delta v}_{[3]}$ for Case (ii) at $n = 3$. Left: Initial velocity range; Right: Final velocity range.

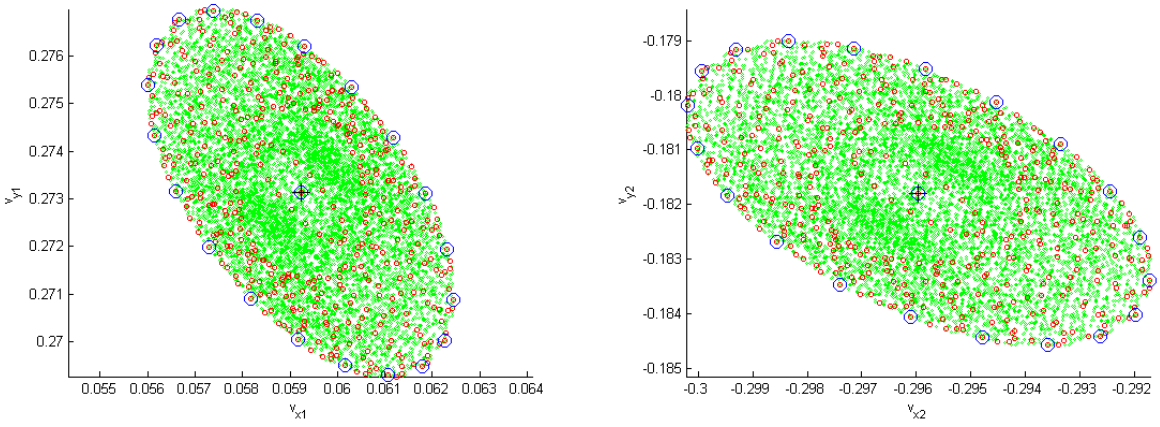

(a) (b)

Fig. 11.: Comparing feasible initial (left) and final (right) velocity range for case (i) for $n = 1$ (blue), $n = 2$ (red) and $n = 3$ (green).

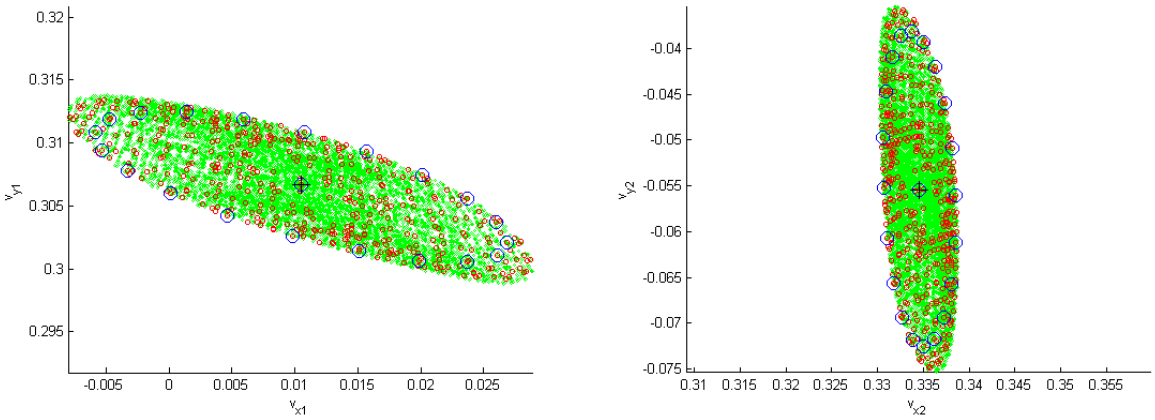

(a) (b)

Fig. 12.: Comparing feasible initial (left) and final (right) velocity range for case (ii) for $n = 1$ (blue), $n = 2$ (red) and $n = 3$ (green).